Weight growth due to resonant simulation particles and a modified δf algorithm with smooth switching between δf and total-f methods

Hong Qin, Ronald C. Davidson, and Edward A. Startsev
Plasma Physics Laboratory, Princeton University, Princeton, New Jersey 08543, USA

(Received 21 January 2008; accepted 14 April 2008; published online 3 June 2008)

When applying the standard δf particle-in-cell simulation method to simulate linear and nonlinear collective instabilities with coherent structures, wave-particle interaction may result in large weight growth for resonant or nearly resonant simulation particles. In this paper, we demonstrate that the large noise associated with the large weight of nearly resonant simulation particles can produce significant error fields at the nonlinear stage of the instability. To overcome this deleterious effect, we have developed a modified δf method that contains a smooth switching algorithm between the δf and total-f methods. Before the switch, the simulation effectively makes use of the desirable low-noise feature of the δf method for small weight to accurately follow unstable mode structures. When the weight function becomes large during the nonlinear phase, the low-noise advantage of the δf method ceases to be significant and the simulation is switched to the total-f method to avoid the large noise induced by nearly resonant simulation particles. This algorithm has been successfully applied to simulation studies of the electrostatic Harris instability driven by large temperature anisotropy in high-intensity charged particle beams typical of applications in high current accelerators, including high-energy density physics and heavy ion fusion. © *2008 American Institute of Physics*. [DOI: 10.1063/1.2920201]

I. INTRODUCTION

The perturbative particle simulation method (δf method) has become an effective low-noise particle-in-cell (PIC) algorithm for simulation studies of collective dynamics of plasmas in application areas ranging from magnetic fusion plasmas[1–8] to high-intensity charged particle beams.[9–13] Recently, there has been a renewed interest in the question of growing weight and associated simulation noise in δf PIC simulations of gradient-driven transport phenomena in magnetic fusion plasmas.[3,4,7,8,14–16] The growing weight in this class of applications is caused by the fact that there in no exact steady state for collisionless plasmas which supports heat and/or particle flux. In this paper, we report another mechanism through which the weight function and the associated noise in the standard δf algorithm can become large, and we propose a modified δf algorithm to ameliorate this deleterious effect. We show that wave-particle resonance between a simulation particle and a coherent mode structure can result in a large weight growth for that simulation particle, which in turn creates a large local error field in the simulation. The modified δf algorithm we have developed can smoothly switch to the total-f method when the weight becomes large during the nonlinear phase of the instabilities under investigation. The concept and algorithms are illustrated through the numerical example of the electrostatic Harris instability driven by large temperature anisotropy in high-intensity charged particle beams, typical of applications in high current accelerators, including high-energy density physics and heavy ion fusion. It is worthwhile to point out that the weight growth mechanism due to resonant simulation particles is effective only for the interaction dynamics with coherent structures. When the system is in a fully developed turbulent state which contains a broad spectrum of modes, the resonance mechanism inducing weight growth is unlikely to be prominent. This paper is organized as follows. The basic mechanism of large weight growth due to resonant simulation particles is discussed in Sec. II. The modified δf algorithm is introduced in Sec. III, and illustrative numerical examples are presented in Sec. IV.

II. LARGE WEIGHT GROWTH DUE TO RESONANT AND NEARLY RESONANT SIMULATION PARTICLES

In the present study, the Vlasov–Maxwell equations for collisionless plasma are given by

$$\left\{\frac{\partial}{\partial t}+\mathbf{v}\cdot\frac{\partial}{\partial \mathbf{x}}+\left[\mathbf{F}_{ext}+\frac{q}{m}\left(\mathbf{E}+\frac{\mathbf{v}\times\mathbf{B}}{c}\right)\right]\cdot\frac{\partial}{\partial \mathbf{v}}\right\}f(\mathbf{x},\mathbf{v},t)=0, \tag{1}$$

$$\nabla\cdot\mathbf{E}=4\pi\int d^3v\,qf(\mathbf{x},\mathbf{v},t), \tag{2}$$

$$\nabla\times\mathbf{B}=\frac{4\pi}{c}\int d^3v\,q\mathbf{v}f(\mathbf{x},\mathbf{v},t)+\frac{1}{c}\frac{\partial\mathbf{E}}{\partial t}, \tag{3}$$

$$\nabla\times\mathbf{B}=-\frac{1}{c}\frac{\partial\mathbf{E}}{\partial t}, \tag{4}$$

$$\nabla\cdot\mathbf{B}=0, \tag{5}$$

where f is the distribution function of particles in phase space, q and m are the particles' charge and mass, and $\mathbf{F}_{ext}$ is the externally applied force. In the quantities f, q, m, $\mathbf{F}_{ext}$, and the velocity integrals over f occurring in Eqs. (1) and

(3), the species index has been suppressed to simplify the notation. The electromagnetic fields $(\mathbf{E},\mathbf{B})$ are determined self-consistently in terms of f. Equations (1)–(5) are written for nonrelativistic dynamics in an inertial reference frame, whose relativistic generalization in flat spacetime is straightforward. Moreover, Eqs. (1)–(5) are applicable to one-component non-neutral plasmas and intense beams, as well as to multispecies plasmas.

In the standard δf method, the distribution function f and the fields are split into two parts,

$$f = f_0 + \delta f = f_0 + wF, \tag{6}$$

$$\mathbf{E} = \mathbf{E}_0 + \delta\mathbf{E}, \tag{7}$$

$$\mathbf{B} = \mathbf{B}_0 + \delta\mathbf{B}, \tag{8}$$

where $(f_0,\mathbf{E}_0,\mathbf{B}_0)$ is a solution of the Vlasov–Maxwell equations, and $(\delta f,\delta\mathbf{E},\delta\mathbf{B})$ are the perturbed distribution function and fields relative to $(f_0,\mathbf{E}_0,\mathbf{B}_0)$. The known solution $(f_0,\mathbf{E}_0,\mathbf{B}_0)$ is allowed to depend on time, even though in most applications it is taken to be a known equilibrium solution with $\partial/\partial t=0$. The perturbed distribution function $\delta f \equiv wF$ is constructed from the distribution function of simulation particles F and the weight function w in phase space. Because the simulation particles follow the same trajectories as the physical particles, F satisfies the Vlasov equation (1) as well. But F need not to be the same as f, and does not necessarily satisfy the Maxwell equations (2)–(5). Some straightforward algebra shows that the dynamics of w is determined from

$$\frac{dw}{dt} = \frac{1}{F}\frac{df_0}{dt} = \frac{q}{m}\left(\delta\mathbf{E} + \frac{\mathbf{v}\times\delta\mathbf{B}}{c}\right)\cdot\frac{1}{F}\frac{\partial f_0}{\partial\mathbf{v}}$$
$$= \frac{w-g}{f_0}\frac{df_0}{dt} = \frac{q}{m}\left(\delta\mathbf{E} + \frac{\mathbf{v}\times\delta\mathbf{B}}{c}\right)\cdot\frac{(w-g)}{f_0}\frac{\partial f_0}{\partial\mathbf{v}}, \tag{9}$$

where $g \equiv f/F$ is a constant of the motion for each simulation particle, i.e., $dg/dt=0$, because $df/dt=0$ and $dF/dt=0$. Therefore, g is determined from the initial conditions of the simulation particles. If F is initially the same as f, then $g\equiv 1$ and the distributions of physical particles and simulation particles are the same. The Maxwell equations for the perturbed fields $(\delta\mathbf{E},\delta\mathbf{B})$ are

$$\nabla\cdot\delta\mathbf{E} = 4\pi\int d^3v\, qwF(\mathbf{x},\mathbf{v},t), \tag{10}$$

$$\nabla\times\delta\mathbf{B} = \frac{4\pi}{c}\int d^3v\, q\mathbf{v}wF(\mathbf{x},\mathbf{v},t) + \frac{1}{c}\frac{\partial}{\partial t}\delta\mathbf{E}, \tag{11}$$

$$\nabla\times\delta\mathbf{B} = -\frac{1}{c}\frac{\partial}{\partial t}\delta\mathbf{E}, \tag{12}$$

$$\nabla\cdot\delta\mathbf{B} = 0. \tag{13}$$

Equations (9)–(13) are exactly equivalent to the nonlinear Vlasov–Maxwell equations (1)–(5). No approximation has been made in the derivation of Eqs. (9)–(13).

We note that the δf method of the gyrokinetic system[17,18] for magnetized plasmas will take a different form from Eq. (9),[1–4,8,15,16] because the gyrocenter coordinate system is nonfibered.[19] We focus here only on the Vlasov–Maxwell system (1)–(5) in standard phase-space coordinate systems (fibered phase-space coordinates), which is valid for both magnetized and unmagnetized plasmas.

In the simulations, the weight function w is carried by each simulation particle and advanced according to Eq. (9). The rate of change of w is evaluated at the phase-space location of the simulation particle. Under certain circumstances, the relative phase between $(\delta\mathbf{E}+\mathbf{v}\times\delta\mathbf{B}/c)$ and $\partial f_0/\partial\mathbf{v}$ can be "locked-in" for some simulation particles for an extended period of time. If this resonant interaction occurs, the weight for these resonant particles may approach g or a negative value with large absolute value, depending on the sign of the locked-in phase. For purposes of illustration, let us study the electrostatic case. We also assume $g=1$ and take f_0 to be locally Maxwellian, i.e.,

$$f_0 = \frac{n_0(\mathbf{x})}{(2\pi T/m)^{3/2}}\exp\left(-\frac{v^2}{2T/m}\right). \tag{14}$$

Under these assumptions, Eq. (9) reduces to

$$\frac{d}{dt}\ln(1-w) = \frac{q}{T}\delta\mathbf{E}\cdot\mathbf{v}, \tag{15}$$

which gives

$$w(t) = 1 - [1 - w(t=0)]\exp[h(t)], \tag{16}$$

$$h(t) = -\int_0^t \frac{q\delta\mathbf{E}\cdot\mathbf{v}}{T}dt. \tag{17}$$

When the phase between $\delta\mathbf{E}$ and $\mathbf{v}$ is locked-in, w approaches 1 if $q\delta\mathbf{E}\cdot\mathbf{v}$ is positive, and w approaches $-\infty$ if $q\delta\mathbf{E}\cdot\mathbf{v}$ is negative. For example, such a resonance can occur linearly between a wave structure and a simulation particle if the velocity of the particle is the same as the phase velocity of the wave. Of course, this picture of exact resonance is only an approximation. The linear resonance can be eliminated by particle acceleration, and the w will not become 1 or $-\infty$, even though nonlinear trapping is still a possible scenario for w to continue to approach the limiting values. Furthermore, in practical numerical simulations, the limiting values of w will not be observed because there are no exactly resonant simulation particles for a finite number of simulation particles, unless they are intentionally loaded in. An arbitrarily loaded simulation particle will generally be located a finite distance from the exact resonance condition.

What is more meaningful is to investigate the behavior of w for a nearly resonant simulation particle. We take

$$\frac{q\delta\mathbf{E}\cdot\mathbf{v}}{T} = k\delta\sin(kx-\omega t)v, \tag{18}$$

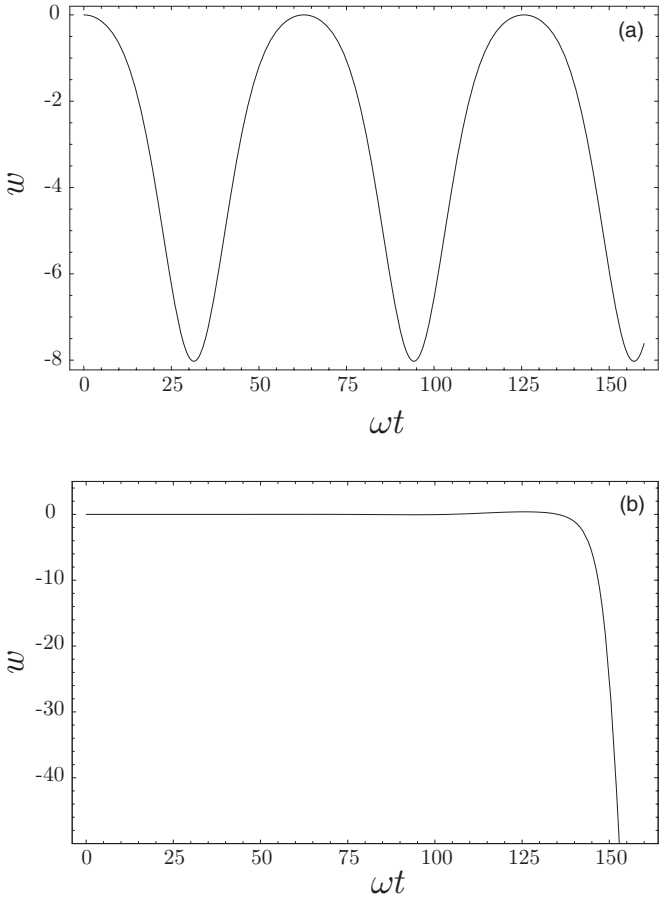

FIG. 1. Weight function of a nearly resonant simulation particle for the case of (a) a constant amplitude wave structure $\delta=0.1$, $\Delta=0.1$, and $x_0=0$ and (b) an unstable wave with $\gamma=0.07\omega$.

$$v=(\Delta+1)\frac{\omega}{k},\quad x=x_0+vt, \tag{19}$$

where (ω,k) is the frequency and wavenumber of the perturbed field, δ is the normalized strength of the field perturbation, and Δ is a measure of the distance from the exact resonance condition. Then Eq. (17) gives

$$h(t)\equiv\frac{\delta(1+\Delta)}{\Delta}[\cos(kx_0)-\cos(kx_0+\Delta\omega t)]. \tag{20}$$

The minimum value of w determined from Eqs. (16) and (20) is approximately

$$w_{\min}\sim-\exp\left(\frac{2\delta}{\Delta}\right). \tag{21}$$

Plotted in Fig. 1(a) is the weight given by Eq. (20) for the case in which $\delta=0.1$, $\Delta=0.1$, and $x_0=0$. We see clearly from Fig. 1(a) that the weight becomes large and negative for a nearly resonant simulation particle. If the mode is unstable, the weight for a nearly resonant particle can be driven to even larger negative values. For example, if we take

$$\frac{q\delta\mathbf{E}\cdot\mathbf{v}}{T}=k\delta\exp(\gamma t)\sin(kx-\omega t)v, \tag{22}$$

where $\gamma>0$, then

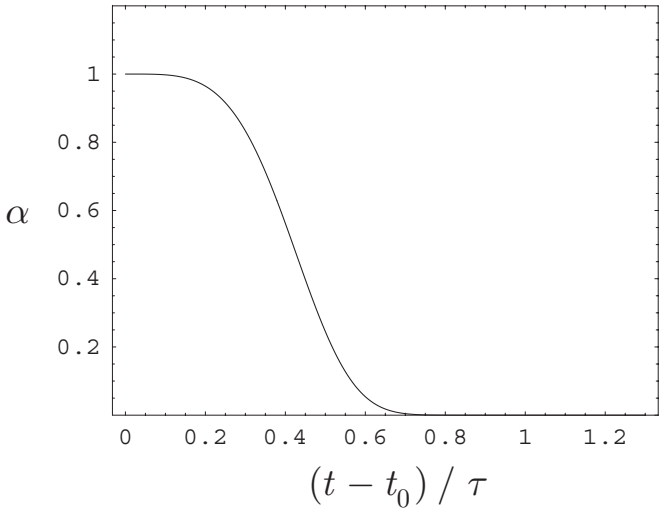

FIG. 2. Switching function $\alpha(t)$ given by Eq. (28) for the case in which $n=3$, $a\tau=90$.

$$h(t)=\frac{\delta\omega(1+\Delta)}{\Delta^2\omega^2+\gamma^2}\{\Delta\omega[\cos(kx_0)-\exp(\gamma t)\cos(kx_0+\Delta\omega t)] + \gamma[\exp(\gamma t)\sin(kx_0+\Delta\omega t)-\sin(k_0x)]\}. \tag{23}$$

Shown in Fig. 1(b) is the weight determined from Eqs. (17) and (23) for the case in which $\delta=0.1$, $\Delta=0.1$, $x_0=0$, and $\gamma=0.07\omega$. The behavior of the weight growth in Fig. 1(b) agrees qualitatively with the numerical simulations for the examples considered in Sec. IV.

When the weight function become large, the low-noise advantage for small weight is diminished, because the noise level in the simulation is proportional to $w^2\sim(\delta f/f)^2$. Larger weight values in the simulations introduce larger noise. In the numerical example presented in Sec. IV, the large noise introduced by the nearly resonant simulation particles produces a large error field, which eventually invalidates the simulation. Theoretically, the allowed range of weights is $-\infty<w\leq1$. The weight is allowed to approach $-\infty$, which corresponds to the case in which $F=0$. Particles with $-\infty<w\ll-1$ do not represent any theoretical difficulty because $\delta f=wF$ should always be finite. For a weight in the range of $-\infty<w\ll-1$, the corresponding value of F is small in size. However, numerically the noise level approaches infinity as $w\rightarrow-\infty$, and such nearly resonant simulation particles are problematic for the reason indicated earlier.

III. MODIFIED δf ALGORITHM WITH SWITCH BETWEEN δf AND TOTAL-f METHODS

To overcome the noise issue brought about by the large weight of nearly resonant simulation particles, we have developed a modified δf method that can switch smoothly between the δf and total-f methods. Before the switch, the simulation still makes effective use of the low-noise feature of the δf method for small weight to follow the detailed evolution of the unstable mode structures. When the weight function becomes large during the nonlinear phase, the

low-noise advantage of the δf method is reduced and the simulation is switched to the total-f method to avoid the large noise induced by nearly resonant simulation particles. In this modified algorithm, the particle's distribution is partitioned as

$$f = \alpha f_0 + wF, \tag{24}$$

where every term in Eq. (24) except for α has the same meaning as in Eq. (6) for the standard δf method. The new feature here is the coefficient α, which is a function of time and can take on values between 0 and 1. The case of $\alpha=0$ corresponds to the total-f method, and the case of $\alpha=1$ corresponds to the standard δf method. The perturbed fields are determined from the perturbed Maxwell equations using the perturbed distribution, which is constructed from α, w, and F as

$$\delta f = (\alpha - 1) f_0 + wF. \tag{25}$$

It is straightforward to show that the governing equation for the evolution of w is given by

$$\frac{dw}{dt} = \frac{w-g}{f_0}\frac{df_0}{dt} + \frac{w-g}{\alpha}\frac{d\alpha}{dt} = \frac{q}{m}\left(\delta \mathbf{E} + \frac{\mathbf{v}\times\delta\mathbf{B}}{c}\right)\cdot\frac{(w-g)}{f_0}\frac{\partial f_0}{\partial \mathbf{v}} + \frac{w-g}{\alpha}\frac{d\alpha}{dt}. \tag{26}$$

Compared with Eq. (9) for the standard δf method, the dynamics of w is now coupled to that of α, which can be either prescribed or determined from some rules coupled back to the amplitude of w. When α varies smoothly from 1 to 0 during the simulation, the δf method is smoothly switched to the total-f method. The coefficient α can also be allowed to depend on phase-space coordinates, and the extra freedom associated with α is introduced to achieve some additional numerical advantages. In the present study, α is chosen to depend only on time t to realize a smooth switch for all simulation particles simultaneously. If the dynamics of α is chosen to depend on the phase-space coordinates as well, then different simulation particles will be switched at different time.

There are many ways to select the function $\alpha(t)$ to achieve the desired switching from the δf method to the total-f method; however, the simulation results should be independent of how the switch function is selected, because the system of equations is always equivalent to the original Vlasov–Maxwell equations. For example, we can choose the switch function to satisfy

$$\frac{d\ln\alpha}{dt} = \begin{cases} 0, & t-t_0<0, \\ -a\left(\dfrac{t-t_0}{\tau}\right)^n, & 0\le t-t_0<\tau, \\ -a, & \tau<t-t_0, \end{cases} \tag{27}$$

which gives

$$\alpha = \begin{cases} 1, & t-t_0<0, \\ \exp\left\{-\dfrac{a\tau}{n+1}\left(\dfrac{t-t_0}{\tau}\right)^{n+1}\right\}, & 0\le t-t_0<\tau, \\ \exp\left\{-\dfrac{a\tau}{n+1}-a(t-t_0-\tau)\right\}\simeq 0, & \tau<t-t_0. \end{cases} \tag{28}$$

Here, t_0 is the starting time of the switch, and τ is the duration of the switch. The starting time t_0 can be either prescribed before the simulation started or the switching can be triggered automatically when the weight growth reaches a certain threshold. The power index n and amplitude parameter a in Eqs. (27) and (28) are chosen to satisfy $a\tau/(n+1)\gg 1$, so that $\alpha\simeq 0$ after the switching $(t-t_0>\tau)$. An example of $\alpha(t)$ given by Eq. (28) is plotted in Fig. 2 for the case in which $n=3$, $a\tau=90$.

The dynamics of α prescribed in Eq. (27) imposes a constant drive, smoothly ramped-up from $t=t_0$, for the weight function to approach $w=g=f/F$, which is the total-f method. Our previous studies of the Harris instability had implemented a rapid switch from the δf method to the total-f method.[12,13] It is now clear that such a rapid switch would be consistent with a singular drive in Eq. (27), which provides a source of numerical discontinuity in the simulation.

IV. NUMERICAL EXAMPLE OF ELECTROSTATIC HARRIS INSTABILITY DRIVEN BY STRONG TEMPERATURE ANISOTROPY

In this section, we give numerical examples of the weight growth due to nearly resonant simulation particles and the modified δf method using the electrostatic Harris instability driven by strong temperature anisotropy in high-intensity charged particle beams. Our main objective here is limited to the demonstration of the weight growth issue and the effectiveness of the switching algorithm. Detailed physics studies of the Harris instability in high-intensity beams using the new switching algorithm will be presented in future publications. We consider a single-species, long coasting beam confined in the transverse (x,y) directions by an applied smooth-focusing force

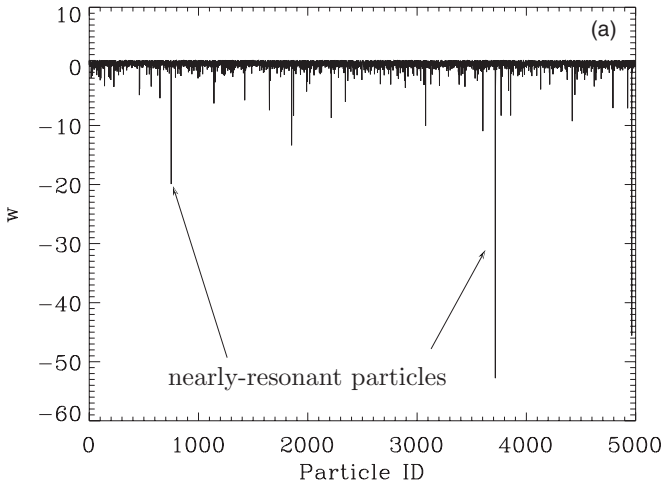

FIG. 3. (a) Weight for 5000 randomly chosen simulation particles at $t=262/\omega_\perp$ using the standard δf method. (b) Weight time history of a nearly resonant simulation particle.

$$\mathbf{F}_{ext} = -m\omega_\perp^2 \mathbf{x}_\perp . \tag{29}$$

Here, $\omega_\perp$ is the constant transverse applied focusing frequency in the smooth-focusing approximation, and $\mathbf{x}_\perp = x\mathbf{e}_x + y\mathbf{e}_y$. In the beam frame, the dynamics of the coasting beam is described by the electrostatic nonlinear Vlasov–Poisson equations[20]

$$\left\{ \frac{\partial}{\partial t} + \mathbf{v}\cdot\frac{\partial}{\partial \mathbf{x}} - \left[\omega_\perp^2 \mathbf{x}_\perp + \frac{q}{m}\nabla\phi \right]\cdot\frac{\partial}{\partial \mathbf{v}} \right\} f(\mathbf{x},\mathbf{v},t) = 0, \tag{30}$$

$$\nabla^2\phi = -4\pi \int d^3v\, qf(\mathbf{v},\mathbf{p},t). \tag{31}$$

Equations (30) and (31) are a special case of the nonlinear Vlasov–Maxwell system (1)–(5).

Energy anisotropy develops naturally in charged particle beams due to phase-space volume conservation when the beam is accelerated. The large temperature anisotropy characteristic of charged particle beams in particle accelerators has long been thought of as a possible free energy source to drive collective instabilities. Recently, a systematic study

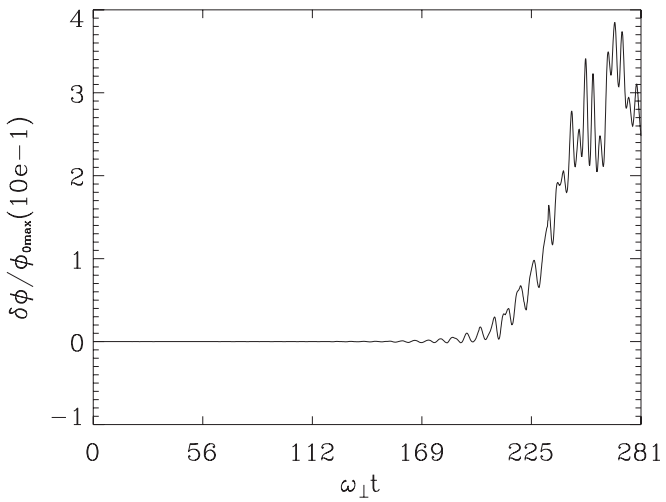

FIG. 4. Potential perturbation at one spatial location using the standard δf method. The simulation result is accurate during the unstable linear growth phase before $t=180/\omega_\perp$, but is dominated by large error fields introduced by the noise associated with the large weight for nearly resonant simulation particles during the nonlinear phase after $t=200\omega_\perp$.

was carried out for this instability,[12,13,21–23] showing that both sufficiently large temperature anisotropy and sufficiently large beam intensity are required for instability to occur. The instability is essentially an electrostatic Harris instability driven by the coupling between the transverse and longitudinal particle dynamics. To simulate the instability using the δf method, we choose the equilibrium f_0 in the beam frame to be the anisotropic thermal equilibrium distribution

$$f_0 = \frac{\hat{n}}{(2\pi m T_\perp)(2\pi m T_z)^{1/2}} \exp\left(-\frac{H_\perp}{T_\perp} - \frac{H_z}{T_z} \right). \tag{32}$$

$$H_\perp = \frac{1}{2}mv_\perp^2 + \frac{m}{2}\omega_\perp^2 r^2 + q\phi_0(r), \quad H_z = \frac{1}{2}mv_z^2. \tag{33}$$

Here, $\hat{n}$=const is the on-axis ($r=0$) number density of beam particles, and $T_\perp$ and T_z are the constant transverse and longitudinal temperatures, respectively. The equilibrium potential $\phi_0(r)$ is determined from Poisson's equation,

$$\nabla^2\phi_0 = -4\pi q\hat{n} \exp\left[-\frac{m\omega_\perp^2 r^2 + q\phi_0}{2T_\perp} \right], \tag{34}$$

which is to be solved numerically inside a perfectly conducting cylindrical pipe with wall radius r_w. The numerical example considered here corresponds to a high-intensity charged particle beam with normalized beam intensity $\omega_p^2/2\omega_\perp^2 = 4\pi\hat{n}e^2/2m\omega_\perp^2 = 0.8$ and temperature anisotropy $T_z/T_\perp = 1/36$. The rms beam radius is $r_b = 0.28 r_w$.

The standard δf method has been applied successfully to simulate the linear phase of the instability, and important physics features, such as the mode structures and growth rates, have been systematically recovered.[12,13,21–23] The low-noise property of the δf method is indispensable in these studies. However, when the simulation is carried out extending into the nonlinear phase, large weight growth due to the nearly resonant simulation particles is observed. Plotted in Fig. 3(a) is the weight function for 5000 randomly chosen

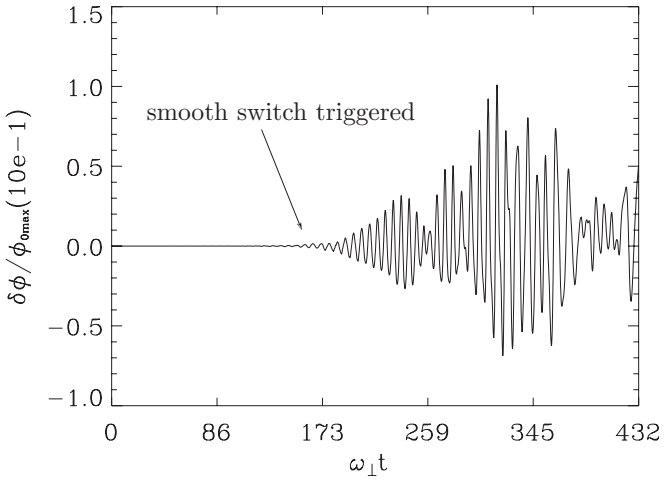

FIG. 5. Potential perturbation at one spatial location using the modified δf method with a smooth switch.

simulation particles at $t=262/\omega_\perp$, where large-amplitude weights for some simulation particles are evident. Analysis shows that the large weights are produced by the resonance between particles and the unstable wave structure in the transverse direction. Plotted in Fig. 3(b) is the time history of the weight for one of the nearly resonant simulation particles. The weight growth before $t=240/\omega_\perp$ agrees qualitatively with the theoretical estimate given in Fig. 1(b) and obtained from Eq. (23). Even though the population of nearly resonant simulation particles is relatively small, the noise associated with the large weights can still generate large error fields locally. The simulation results for the perturbed potential at one spatial location are presented in Fig. 4, from which we observe that the simulation is accurate for the unstable linear growth before $t=180/\omega_\perp$, and valuable information about the instability has been generated. However, the signal during the nonlinear phase after $t=200/\omega_\perp$ is dominated by the error fields, and the simulation crashes shortly after $t=280/\omega_\perp$.

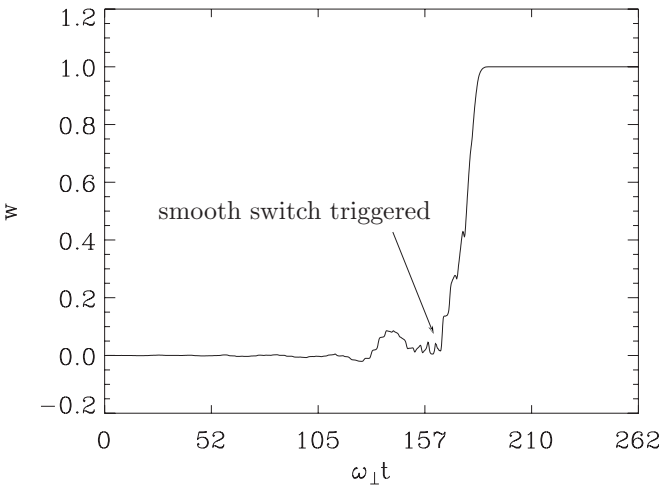

FIG. 6. Weight history of the same nearly resonant simulation particle as in Fig. 3(b) using the modified δf algorithm.

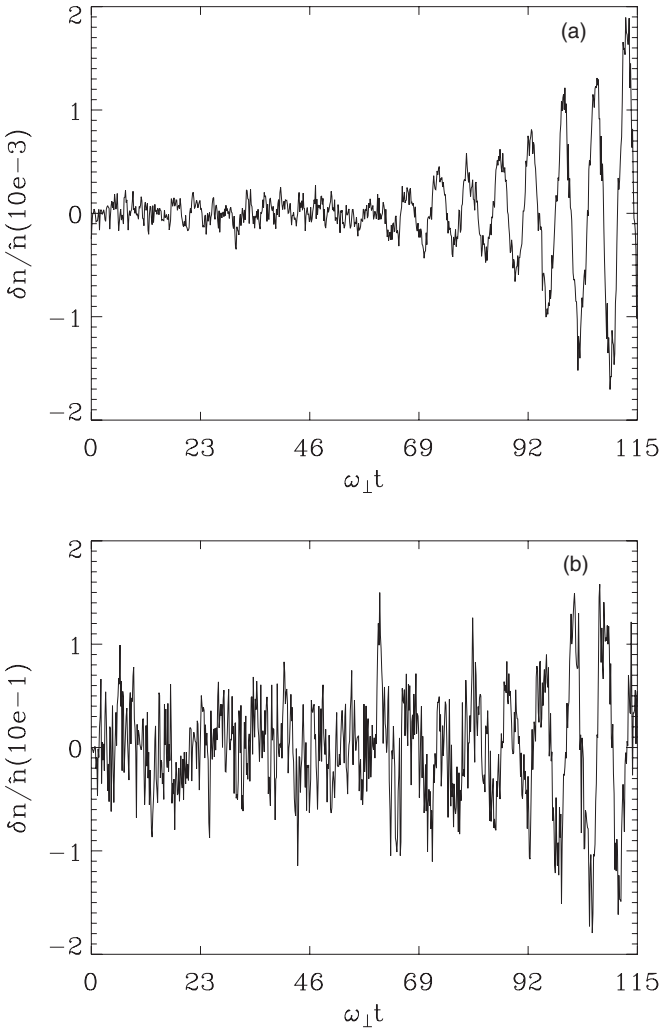

FIG. 7. Density perturbation from $t=0$ to $t=115/\omega_\perp$ using the δf method (a) and the total-f method (b).

Valid simulation results for both the linear and nonlinear phases have been obtained using the modified δf algorithm with the switch between the standard δf and total-f methods described in Sec. III. Show in Fig. 5 is the time history of the perturbed potential at the same location as in Fig. 4. The smooth switch in the form of Eq. (27) with $n=3$, $\tau=30/\omega_\perp$, and $a=3\omega_\perp$ is automatically triggered when the maximum absolute value of weight for all particles is larger than 1. In this simulation, the switch is triggered at $t=t_0=162/\omega_\perp$. We can clearly identify the well-behaved linear growth and nonlinear saturation dynamics in Fig. 5. The fact that the switching algorithm can eliminate the deleterious weight growth for the nearly resonant simulation particles is clearly demonstrated in Fig. 6, which shows the time history of the weight for the same nearly resonant simulation particle as in Fig. 3(b). After the switch is turned on, the weight function smoothly approaches 1 and the simulation method is thereafter switched to the total-f method during the nonlinear phase. Before the deleterious weight growth becomes significant, it is advantageous to use the δf method to reduce the simulation noise. If we start to use the total-f method from the very beginning, then the simulation is dominated by dis-

crete particle noise before the unstable coherent structure is able to grow. Plotted in Fig. 7 is the comparison between the density perturbation by the δf method and the total-f method from $t=0$ to $t=115/\omega_{\perp}$. The initial density perturbation imposed for both cases is at the 10^{-4} level. Figure 7(b) shows that the simulation result using the total-f method is dominated by the discrete particle noise at the 10^{-2} level, which is determined by the number of simulation particles per cell (about 100) in the simulation. On the other hand, the simulation result in Fig. 7(a) using the δf method is able to capture the instability at the initial linear phase when the perturbation level is still small.

V. CONCLUSIONS AND FUTURE WORK

When applying the standard δf PIC simulation method to simulate nonlinear collective dynamics with coherent structures, wave-particle resonance may result in large weight growth for resonant or nearly resonant simulation particles. Using the example of the electrostatic Harris instability driven by large temperature anisotropy in high-intensity beams typical of applications in high current accelerators, including high-energy density physics, and heavy ion fusion, we have demonstrated that the large noise associated with the large weight of nearly resonant simulation particles can produce significant error fields at the nonlinear stage of the instability. To overcome this difficulty, we have developed a modified δf method that contains a smooth switching algorithm between the δf and total-f methods. Before the switch, the simulation still effectively makes use of the low-noise feature of the δf method for small weight to follow accurately the unstable mode structures. When the weight function becomes large during the nonlinear phase, the low-noise advantage of the δf method ceases to be prominent and the simulation is switched to the total-f method to avoid the large noise induced by nearly resonant simulation particles. This algorithm has been successfully applied to simulation studies of the electrostatic Harris instability driven by large temperature anisotropy. In this paper, we have only reported the use of the modified δf algorithm to realize a simultaneous, smooth switch for all of the simulation particles from the δf method to the total-f method. However, the method developed in Sec. III is much more general. The switching function α in Eq. (27) can be allowed to depend on phase-space coordinates, which implies that the switch for different simulation particles can be turned on at different times, depending on the phase-space locations of the simulation particles. Another possible application is to use the algorithm to switch back to the δf method from the total-f method. This capability is desirable when the dynamical system reaches a new quasi-steady-state, and the construction of a new unperturbed solution can be numerically beneficial. Progress in these directions will be reported in future publications.

ACKNOWLEDGMENTS

We are grateful to Dr. Weixing Wang, Dr. Wei-li W. Lee, and Dr. John Krommes for fruitful discussions.

This research was supported by the U. S. Department of Energy under Contract No. AC02-76CH03073.

[1] S. E. Parker and W. W. Lee, Phys. Fluids B **5**, 77 (1993).
[2] G. Hu and J. A. Krommes, Phys. Plasmas **1**, 863 (1994).
[3] Y. Chen and S. E. Parker, J. Comput. Phys. **189**, 463 (2003).
[4] W. M. Nevins, G. W. Hammett, A. M. Dimits, W. Dorland, and D. E. Shumaker, Phys. Plasmas **12**, 122305 (2005).
[5] W. M. Nevins, J. Candy, S. Cowley, and T. Dannert, Phys. Plasmas **13**, 122306 (2006).
[6] W. X. Wang, Z. Lin, W. M. Tang, W. W. Lee, S. Ethier, J. L. V. Lewandowski, G. Rewoldt, T. S. Hahm, and J. Manickam, Phys. Plasmas **13**, 092505 (2006).
[7] W. M. Nevins, S. E. Parker, Y. Chen, J. Candy, A. Dimits, W. Dorland, G. W. Hammett, and F. Jenko, Phys. Plasmas **14**, 084501 (2007).
[8] Y. Chen and S. E. Parker, Phys. Plasmas **14**, 082301 (2007).
[9] H. Qin, R. C. Davidson, and W. W. Lee, Phys. Rev. ST Accel. Beams **3**, 084401 (2000).
[10] H. Qin, Phys. Plasmas **10**, 2078 (2003).
[11] H. Qin, E. A. Startsev, and R. C. Davidson, Phys. Rev. ST Accel. Beams **6**, 014401 (2003).
[12] E. A. Startsev, R. C. Davidson, and H. Qin, Phys. Plasmas **9**, 3138 (2002).
[13] E. A. Startsev, R. C. Davidson, and H. Qin, Phys. Rev. ST Accel. Beams **6**, 084401 (2003).
[14] W. W. Lee and W. M. Tang, Phys. Fluids **31**, 612 (1988).
[15] T. G. Jenkins and W. W. Lee, Phys. Plasmas **14**, 032307 (2007).
[16] J. A. Krommes, Phys. Plasmas **14**, 090501 (2007).
[17] H. Qin, R. H. Cohen, W. M. Nevins, and X. Q. Xu, Phys. Plasmas **14**, 056110 (2007).
[18] H. Qin, Fields Inst. Commun. **46**, 171 (2005).
[19] H. Qin and W. M. Tang, Phys. Plasmas **11**, 1052 (2004).
[20] R. C. Davidson and H. Qin, *Physics of Intense Charged Particle Beams in High Energy Accelerators* (World Scientific, Singapore, 2001).
[21] E. A. Startsev, R. C. Davidson, and H. Qin, Phys. Rev. ST Accel. Beams **8**, 124201 (2005).
[22] E. A. Startsev, R. C. Davidson, and H. Qin, Phys. Plasmas **14**, 056705 (2007).
[23] H. Qin, R. C. Davidson, and E. A. Startsev, Phys. Rev. ST Accel. Beams **10**, 064201 (2007).